Journal of Structural Biology 184 (2013) 375–378

Contents lists available at ScienceDirect

Journal of Structural Biology

journal homepage: www.elsevier.com/locate/yjsbi

Crystallization Notes

Metal-mediated crystallization of the xylose transporter XylE from *Escherichia coli* in three different crystal forms

Esben M. Quistgaard [a,*], Christian Löw [a], Per Moberg [a], Pär Nordlund [a,b,*]

[a] Department of Medical Biochemistry and Biophysics, Karolinska Institutet, SE-17177 Stockholm, Sweden
[b] Division of Structural Biology and Biochemistry, School of Biological Sciences, Nanyang Technological University, 138673 Singapore, Singapore

ARTICLE INFO

Article history:
Received 5 September 2013
Accepted 11 September 2013
Available online 21 September 2013

Keywords:
GLUT transporter
Membrane protein crystallization
Metal binding
Cadmium
Crystal packing
Diffraction anisotropy
Protein engineering

ABSTRACT

XylE is a major facilitator (MFS) xylose transporter, which is homologous to the mammalian glucose transporters (GLUT family). We have previously reported the structure of XylE in fully inward open and partially occluded inward open conformations in space groups $P6_1$ and C2, respectively. Here we present the crystallization of a third crystal form, $P2_12_12_1$ (~4 Å resolution), also representing an inward facing conformation, and analyze all three forms in terms of crystallization conditions and packing. The crystallization conditions were generally very similar with only slight changes needed to favor one form over another, e.g. the presence of lanthanide ions greatly favors C2 over $P2_12_12_1$ under otherwise identical conditions. Cadmium was essential for crystallization of all three forms, which indeed all contain a Cd^{2+} ion in a crystal packing interface, though surprisingly in different positions. Cadmium was also found to bind to XylE in solution. The diffraction data were highly anisotropic for all forms, reflecting a lack of ordered crystal contacts along one or two of the cell axes. The best diffracting directions thus consistently correlate with the presence of ordered contacts, most of which are metal-mediated. The data presented here highlight the utility of metal ions in membrane protein crystallization and suggest that metal site engineering may be a productive path towards obtaining additional crystal forms of XylE and other membrane proteins.

The major facilitator (MFS) superfamily represents the largest superfamily of secondary active transporters. It is found in all branches of life and has diversified into numerous families with diverse substrate specificities (Pao et al., 1998). In general, MFS transporters consist of 12 transmembrane helices organized into two structurally similar 6-helical subdomains, which cradle the substrate binding site (Yan, 2013). They are believed to function by an alternate access mechanism (Jardetzky, 1966) where the two subdomains move relative to each other during the transport cycle to expose the binding site to either the cytoplasm (inward open state), or the extracellular environment (outward open state), or to occlude it from both sides (occluded state). At present, structures are known of all these states (Yan, 2013), but progress in understanding the transport mechanism has been hampered by the fact that no cases were known where the same MFS transporter has been crystallized in more than one state. This has however recently changed with the structure determination of XylE, a D-xylose:H^+ symporter from *Escherichia coli*, which is related to the mammalian glucose transporters (GLUT family) (Davis and Henderson, 1987). Thus, three structures have been determined in a slightly outward open occluded conformation in complex with either xylose, glucose or brominated glucose at 2.6–2.9 Å resolution (Sun et al., 2012), and two different inward facing structures have been determined; fully inward open (anisotropic 4.2 Å resolution) and partially occluded inward open (anisotropic 3.8 Å resolution) (Quistgaard et al., 2013). This has opened up unprecedented opportunities for mechanistic studies, but capturing the transporter in additional states would likely be necessary to fully understand the transport mechanism. In order to achieve this, and perhaps also obtain higher resolution for the inward facing conformations, we believe that it would be instructive to compare the present structures in terms of crystallization conditions and crystal packing. We will mainly focus on the inward facing structures originating from our lab, but will also discuss our findings in context of the outward facing occluded structures.

1. A third crystal form of inward facing XylE

The previously reported structures of inward open and partially occluded inward open XylE were obtained using protein purified in the detergent decyl maltoside (DM) and crystallized in space

* Corresponding authors. Address: Department of Medical Biochemistry and Biophysics, Karolinska Institutet, Scheeles väg 2, SE-171 77 Stockholm, Sweden. Fax: +46 852486850.
E-mail addresses: esben.quistgaard@ki.se (E.M. Quistgaard), par.nordlund@ki.se (P. Nordlund).

1047-8477/$ - see front matter © 2013 Elsevier Inc. All rights reserved.
http://dx.doi.org/10.1016/j.jsb.2013.09.009

groups $P6_1$ and C2, respectively (Quistgaard et al., 2013). Here we present the crystallization of a third crystal form, $P2_12_12_1$, which was grown from selenomethionine labeled protein expressed and purified in DM as described for the other two. The condition for the best crystal was; 36% PEG 400, 100 mM MES pH 6.5, 200 mM NaCl and 10 mM $CdCl_2$. Data were collected at Soleil in France and processed with XDS and XSCALE (Kabsch, 2010) (Supplementary Table 1). Phasing by molecular replacement with single wavelength anomalous dispersion (MR SAD) was readily achieved with Phenix AutoSol (Adams et al., 2010) using the C2 form as search model and data cut at 4.0 Å resolution (higher resolution data could potentially have been included at expense of overall completeness by employing ellipsoidal truncation). The density modified electron density map and the positions of the anomalous difference peaks clearly demonstrate that the protein is captured in an inward facing conformation, which appears to be highly similar to the partially occluded conformation also observed for the C2 form (Supplementary Fig. 1). The model was therefore not refined.

2. Comparison of crystallization conditions for inward facing XylE

The crystallization conditions were highly similar for all three crystal forms. The $P2_12_12_1$ form appeared when using a condition consisting of 25–40% PEG 400, 100 mM MES pH 6.0–6.5, 0–400 mM NaCl and 5–10 mM $CdCl_2$. However, if the NaCl concentration was increased to 500–1000 mM, the $P6_1$ form appeared instead. For this form, the $CdCl_2$ concentration could also be lowered slightly. Conversely, if keeping the NaCl concentration at 0–400 mM, but pre-incubating the protein with 2–5 mM Lu acetate for ~1 h before setting up the crystallization experiment, the C2 crystals appeared. For this form, the pH could also be lowered to 5.5 and Lu acetate could be replaced by any other lanthanide salt that we tested, i.e. various salts of samarium, europium, holmium and praseodymium (Fig. 1). The $P2_12_12_1$ and C2 crystals were quite reproducible and generally appeared and grew fast (maximum size often attained within a week), while $P6_1$ crystals of useful size, i.e. $\geqslant$120 μm, were only rarely obtained and usually grew very slowly (could take months to reach maximum size). It is noteworthy that the presence of cadmium was essential for all forms. We tried replacing it with various other divalent cations, but only with zinc did we also obtain crystals, and these diffracted very poorly. Without either cadmium or zinc present, no crystals of any form could be obtained.

3. Role of metal ions in crystal packing of inward facing XylE

When viewing the crystal packing, it is not surprising that cadmium was found to be essential for crystallization, as it mediates crystal contacts in all three forms (Fig. 2A–C). A characteristic of all tested crystals was the presence of very severe anisotropy in the diffraction data. The reason for this becomes apparent when comparing the crystal packing with the diffraction intensity along the three principle axes as captured by F/sigma versus resolution plots. For the $P6_1$ form, ordered crystal contacts are generated in the a-b plane by two symmetry operators found parallel to the c-axis; the crystallographic 6_1-screw axis and a 3-fold non-crystallographic symmetry (NCS) rotation-axis, on which the Cd^{2+} ion is localized (Fig. 2A). On the other hand, no ordered contacts are found along the c-axis (Fig. 2A). Accordingly, diffraction was much stronger along the a- and b-axes than along the c-axis (Fig. 2D). For the $P2_12_12_1$ form, only one ordered crystal contact could be identified, which is generated by a crystallographic 2_1-screw axis parallel to the c-axis and mediated by the Cd^{2+} ion (Fig. 2B). This remarkable shortage of ordered contacts is reflected in a particularly striking F/sigma versus resolution plot, revealing far better diffraction along the c-axis than either a- or b-axes (Fig. 2E). For the C2 form, a metal-mediated crystal contact is generated in the a-b plane by the 2-fold crystallographic rotation axis, which is found parallel to the b-axis and the C-centering of the lattice. Furthermore, an additional contact is generated by a 2-fold NCS rotation axis that is orthogonal to the a-b plane (Fig. 2C). All ordered contacts are therefore found in the a-b plane, and indeed, diffraction was markedly strongest along the a- and b-axes (Fig. 2F). To sum up, the best diffracting directions were for all crystal forms found to consistently correlate with the presence of ordered contacts, with half ($P6_1$ and C2) or all of these ($P2_12_12_1$) being mediated by metal ions. Interestingly, the Cd^{2+} ion is found in different sites in all forms though always close to His258 (Fig. 3). In the $P6_1$ form it is localized between His258 and His262 where it mediates symmetric trimerization via the third and longest of the cytoplasmic helices from its position on the 3-fold NCS axis (Fig. 3A). In the $P2_12_12_1$ form it is found in an asymmetric site, which is likely composed

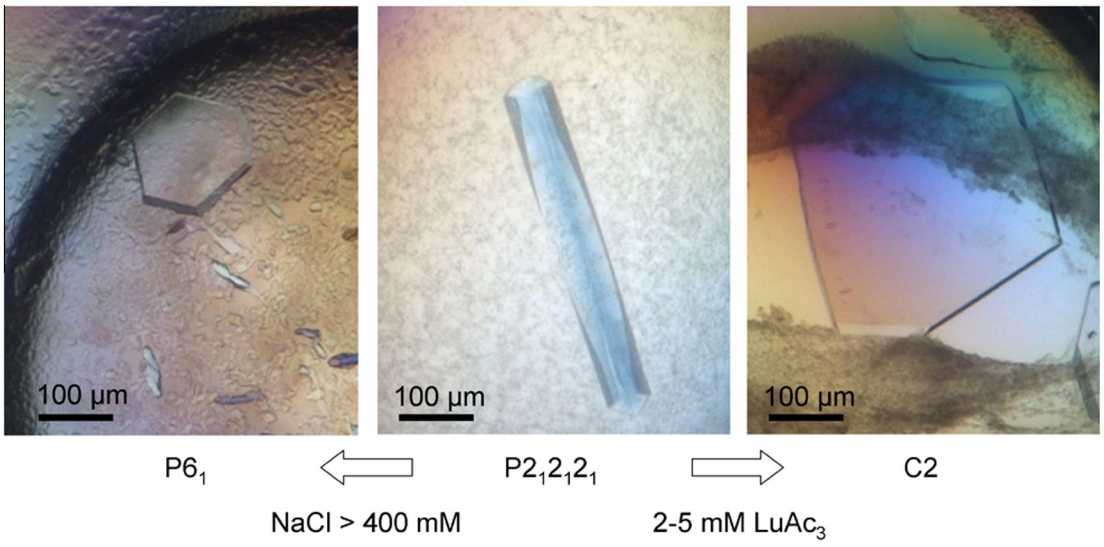

Fig. 1. Morphology of the three different crystal forms. Note however that the morphology of the C2 and $P2_12_12_1$ forms were rather variable. Variations in the $P2_12_12_1$ crystallization condition are given that would lead to either of the other crystal forms.